In Proceedings of the 24th Annual Conference of the IEEE Industrial Electronics Society (IECON'98), p. 1176-1182, □ Aachen, Germany, 31de August- 4 de Set., 1998.

Using Attractor Dynamics to Control Autonomous Vehicle Motion

Estela Bicho
Department of Industrial Electronics,
University of Minho
4800 Guimarães, Portugal
CRNC-CNRS, Ch. Joseph Aiguier, 31
13402 Marseille Cedex 20, France
estela@lnf.cnrs-mrs.fr

Pierre Mallet
CRNC-CNRS, Ch. Joseph Aiguier, 31
13402 Marseille Cedex 20, France
mallet@lnf.cnrs-mrs.fr

Gregor Schöner
CRNC-CNRS, Ch. Joseph Aiguier, 31
13402 Marseille Cedex 20, France
gregor@lnf.cnrs-mrs.fr

Abstract – **Planning collisionless paths for autonomous vehicles is a basic task of autonomous robotics. A large body of work has addressed this issue by starting out from symbolic representations of the environment, in which obstacles and targets are represented metrically. In practice, these representations are difficult to obtain, however. This paper shows that the dynamic approach to path planning (Schöner, Dose, 1992) can be implemented on simple autonomous vehicles using only low-level sensory information such as distances sensed by infra-red or sonar detectors. Each sensor is assumed to contribute a repulsive force-let to a dynamical system, which generates a trajectory of heading direction. The repulsion force is a decreasing function of sensed distance. This leads to obstacle avoidance. Movement toward a target is achieved by adding an attractive force-let. This architecture generates smooth collisionless trajectories based on real-time sensory information.**

I. INTRODUCTION

A basic problem in autonomous robotics is the generation of collision-free vehicle paths that bring the robot system to a specified target location. This problem has been address in theoretical work by isolating the path planning aspect from the aspects of obtaining sensory information about the world and of controlling vehicle motion to generate the path (review, e.g., in Latombe, 1991; Chapters in 4 and 7 in Cox, Wilfong, 1990). Some of these theoretical approaches propose algorithms that guarantee that constraints are fulfilled and that a path is found if one exists (e.g., Kedem, Sharir, 1988). The potential field approach (Khatib, 1986) is a heuristic method that generates smooth paths that facilitate control. The dynamic approach (Schöner, Dose, 1992) makes this linkage to control even stronger by replacing the transient solutions of the potential field approach with attractor solutions of a dynamical system, that therefore contributes to the asymptotic stability of the overall control scheme.

The major drawback of many of these schemes remains, however, that they build on representations of the environment that are exceedingly difficult to obtain in real time. Many of the exact approaches, for instance, rely on polygonal representations of objects in the world. This also poses the problem of the overall control-theoretic stability of the path generation systems, as the step-wise computation of representations of obstacles and targets is not characterized by a time scale.

The goal of the present paper is to demonstrate that the dynamic approach (reviewed in Schöner, Dose, Engels, 1995) can be used to generate collision-free paths toward targets even if the low-level sensory information is used instead of representations of the environment. This extends earlier work by Bicho and Schöner (1997), in which collision-free movement towards maxima of light intensity (photo-taxis) was demonstrated on a low-level platform.

II. THE HARDWARE

The autonomous mobile robot was designed and built by the Dynamical Robotics group at the CRNC-CNRS in Marseille (Figure 1).

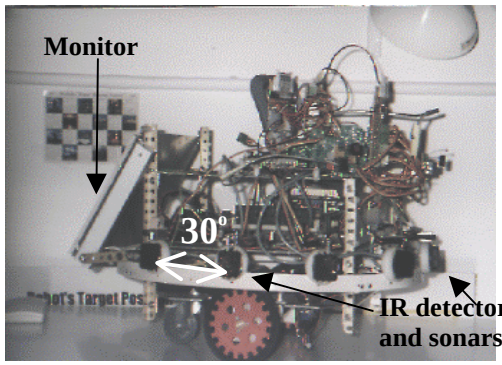

Figure 1. The autonomous mobile robot used in the demonstrations

The vehicle fits approximately into a 40 by 40 by 40 cm cube. It consists of two lateral motorized wheels, and a passive caster wheel, an embedded PC 104 computer system, a number of low-level sensors (sonars, infra-red detectors, photo-resistors), and a radio communication system for remote monitoring. The single-board computer system is based on a 486 DX4 processor operating at 100MHz, is equipped with 4 Mbytes of DRAM and 4 Mbytes of FLASH memory. Its operation system is DOS 6.22 and it was programmable in Qbasic. A monochrome LCD monitor, a removable keyboard and a removable driver for 3 1/2 diskettes makes the platform an autonomous workstation. A radio link between the robot and a second computer is used to monitor the robot's sensory data and the state of its dynamic systems architecture. All control is done on-board. The two lateral wheels are each driven by a DC

brushless servomotor, each separately controlled by electronic circuitry that guarantees accurate control of rotation speed without the use of shaft encoders. The relationship between input voltage and rotation speed is approximately linear, so that generating desired robot's speeds and turning rates is easy. The motors are powered by two 12 Volt batteries in line, with a separate 12 Volt battery supplying the computer and the on-board electronics. This yields on average an autonomy of about 1h 30 min (the computer being the bottleneck).

The demonstrations reported in this paper make use of seven active infrared sensors and seven Polaroid sonar time of flight sensors. Both are used to obtain distance measures. In both cases the angular range over which distances values are averaged by the sensors is about 30°. The sensors are arranged such that their sensitive cones just touch, thus covering completely the forward 180° semicircle. The infrared sensors detect maximal distances of about 0.6 m. Their signal is uncalibrated as it depends on surface reflectivity. The range of the sonars was limited to between 0.45 and 1.75 m to limit sensing time.

III. THE ATTRACTOR DYNAMICS OF HEADING DIRECTION

The dynamic approach to path generation in autonomous vehicles (Schöner, Dose, 1992; Schöner, Dose, Engels, 1995) employs the heading direction, ϕ, relative to some external world axis, as the planning variable. The path plan is a time course of this variable. This time course is obtained from a differential equation of heading direction. Task constraints are component forces of this dynamical system. For example, the directions, ψ_{obs} (relative to a fixed external world axis) in which obstacles lie from the viewpoint of the robot, and similarly, the direction, ψ_{tars} in which the target lies are constraints that are represented by repulsive and attractive force-lets acting on heading direction (Figure 2). At all times, heading direction is in a resulting attractor of this dynamics. As the vehicle moves, the directions to obstacles and target in the world change, so that resultant attractor shifts, pulling heading direction along. Because all angles are measured in an external reference frame, the contributions of the obstacles and the target to the dynamical system of heading direction do not depend on the current orientation of the robot. If the robot is rotated on the spot, the directions to the objects in the world do not change and thus the dynamics of heading direction is independent of the current value of heading direction. Only because this is true does the resultant dynamics have attractors and repellors as designed. How can this approach be applied to our vehicle, which knows nothing about external reference frames, nothing about objects resting in the world, but has only its own low-level sensory information to generate a dynamics of heading direction?

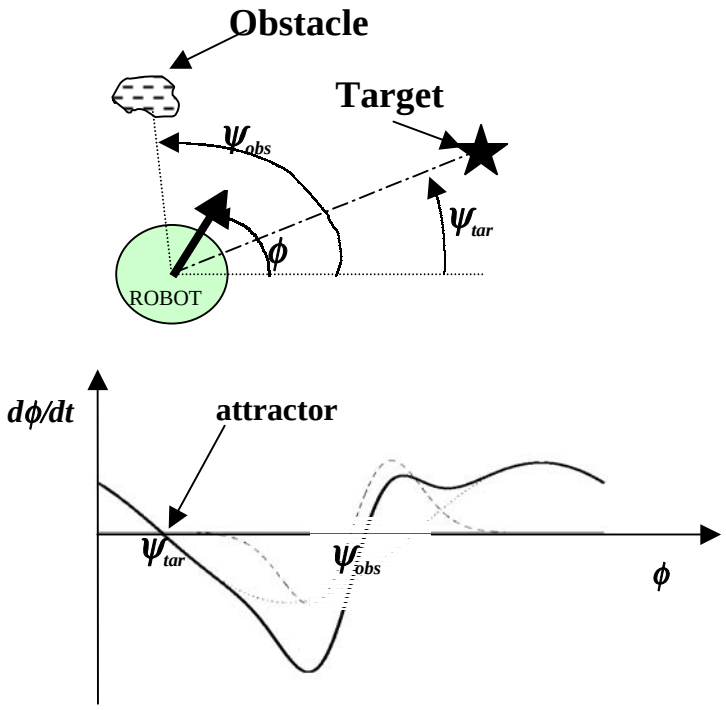

Figure 2. On the top: Constraints for the dynamics of ϕ are the directions at which obstacles and target lie from the current positio of the robot, i.e. directions ψ_{obs} and ψ_{tar} respectively. On the bottom: Resultant attractor from the superposition of the repulsive force-let (traced line) from obstacle constraints and attractive force (doted line) due to target contribution. The resultant dynamics is the continuous bold line. Parameters must be tuned so that the system is relaxed in the attractor.

A. *Obstacle avoidance*

On our low-level platform, each sensor looks into a fixed direction, θ_i, in a reference frame fixed to the robot body. Thus, each sensor looks into a direction, $\psi_i=\phi+\theta_i$, in an external reference frame if ϕ is the heading direction in such an external frame (Figure 3).

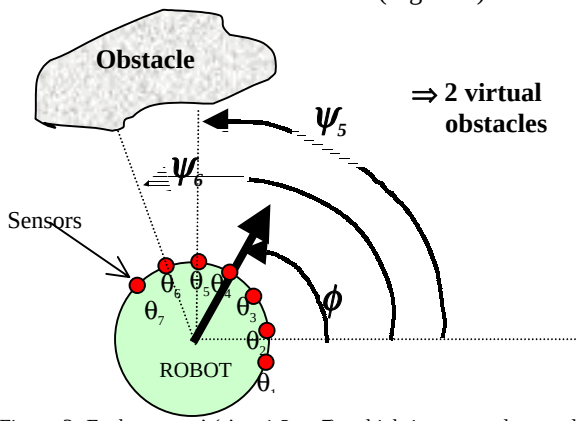

Figure 3. Each sensor i (i = *1,2,…,7*), which is mounted at angle θ_i from the frontal direction, specifies an obstacle at direction $\psi_i = \phi + \theta_i$, in an external reference frame. ϕ is the heading direction in the external reference. In the figure, sensors 5 and 6 specify virtual obstacles at directions ψ_5 and ψ_6 respectively.

Our strategy is now simply to say that each sensor i (i = 1,2,…) specifies a virtual obstacle in that direction ψ_i,

so that repulsive force-lets centered at these directions are erected. Each repulsive force-let reads:

$$f_{obs,i} = \lambda_i(\phi - \psi_i)\exp\left[\frac{(\phi-\psi_i)^2}{2\sigma_i^{\,2}}\right] \qquad (1)$$

In this equation only the difference ϕ-ψ_i =-θ_i, which is fixed, enters into the dynamics of heading direction The strength of repulsion, λ_i, from each virtual obstacle at direction ψ_i is a decreasing function of sensed distance, d_i,:

$$\lambda_i = \beta_1 \exp\left[-\frac{d_i}{\beta_2}\right] \qquad (2)$$

where β_1 controls the maximum repulsion strength of this contribution, and β_2 controls the spatial rate of decay. The range of the force-let sensor sector, $\Delta\theta$ (=30°), but also depends on distance because the angle subtended by half the vehicle at the sensed distance is added on each side of the sensor sector as a safety margin:

$$\sigma_i = \arctan\left[\tan\left(\frac{\Delta\theta}{2}\right) + \frac{R_{robot}}{R_{robot}+d_i}\right] \qquad (3)$$

The contributions from all the sensors are summed. Therefore, the overall obstacle avoidance dynamics reads:

$$\frac{d\phi}{dt} = F_{obs} = \sum_i f_{obs,i} \qquad (4)$$

Figure 4 shows individual repulsive force-lets and their sum for the situation illustrated in Figure 2.

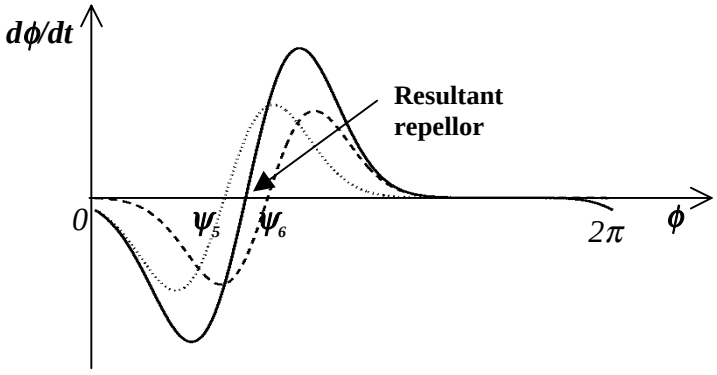

Figure 4. In the situation depicted in Figure 3 two virtual obstacles are detected, at directions ψ_5 and ψ_6. In that figure ϕ=60°, ψ_5 =90° and ψ_6 =120°, sensed distances are 30 and 35 cm respectively. Two repulsive force-lets centered at these directions are therefore erected. Doted line is the force-let at direction ψ_5 while traced line is the force-let at ψ_6. The continuous line shows the resultant dynamics. The resultant repellor is approximately at 103°.

The two sensors responding to the obstacle lead to a single repellor that covers the entire angle subtended by the obstacle. Figure 5 shows how at a different orientation of the sensors relative to the obstacle three sensors respond to the obstacle, leading to changed individual force-lets. Their sum erects a repellor at approximately the same heading direction, however.

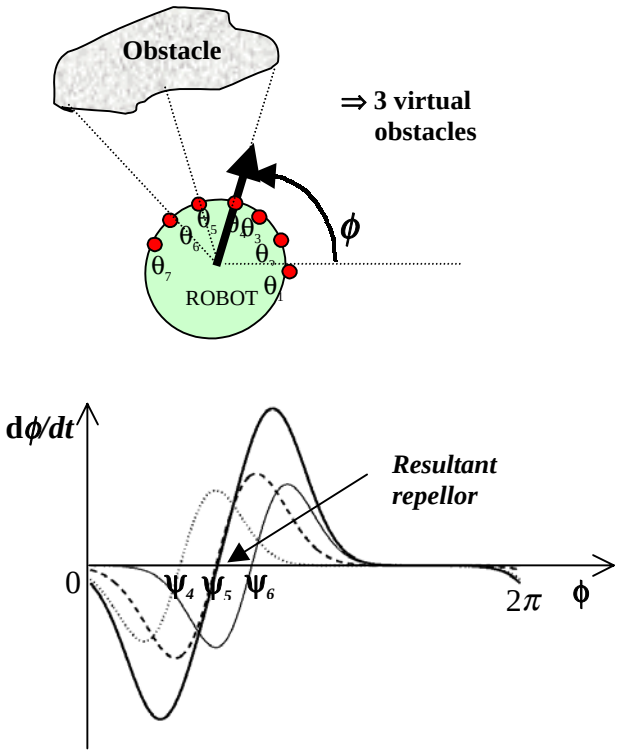

Figure 5. On the top: with respect to figure ´3 robot turned left just $\Delta\theta/2$ (= 15°) degrees. From this rotation results that three virtual obstacles are detected now, at directions ψ_4, ψ_5 and ψ_6. In this figure ϕ=75°, ψ_4 =75° and ψ_5 =105°, distances are 45, 30 and 45 cm respectively. On the bottom: three repulsive force-lets are erected at these directions. The continuous bold line represents the resultant dynamics. Resultant attractor is at 105°.

B. *Target Acquisition*

Targets are given in external coordinates (X_{target},Y_{target}). The robot keeps an estimate of its own location, (X_{robot},Y_{robot}), in the external reference frame by integrating motor commands (dead-reckoning) from an initial reference position. The direction, ψ_{tar}, relative to the world x-axis, in which the target lies as seen from the robot is:

$$\psi_{tar} = \arctan\left(\frac{Y_{tar} - Y_{robot}}{X_{tar} - X_{robot}}\right) \qquad (5)$$

An attractive force-let is defined by:

$$f_{tar} = -\lambda_{tar}\sin(\phi - \psi_{tar}) \qquad (6)$$

The strength of this force-let is weaker than the strength of obstacle avoidance contribution, which thus have priority. Its range extends, however, across the entire 360° domain of heading direction.

The complete heading direction dynamics is obtained summing obstacle and target contributions:

$$\frac{d\phi}{dt} = F_{obs} + f_{tar} \qquad (7)$$

In Figure 6 illustrates the simultaneous effect of target and obstacle constraints. In the shown situation, the

space between the two obstacles is not sufficient for the robot to pass through them. The target lies behind this opening, the most challenging situation for obstacle avoidance. The obstacle avoidance contribution to the dynamics (doted line) exhibits a repellor at the direction in between the two obstacles, while the target contribution (dashed line) erects an attractor there. The resultant dynamics (solid line) has a repellor at this location because the obstacle contributions dominate.

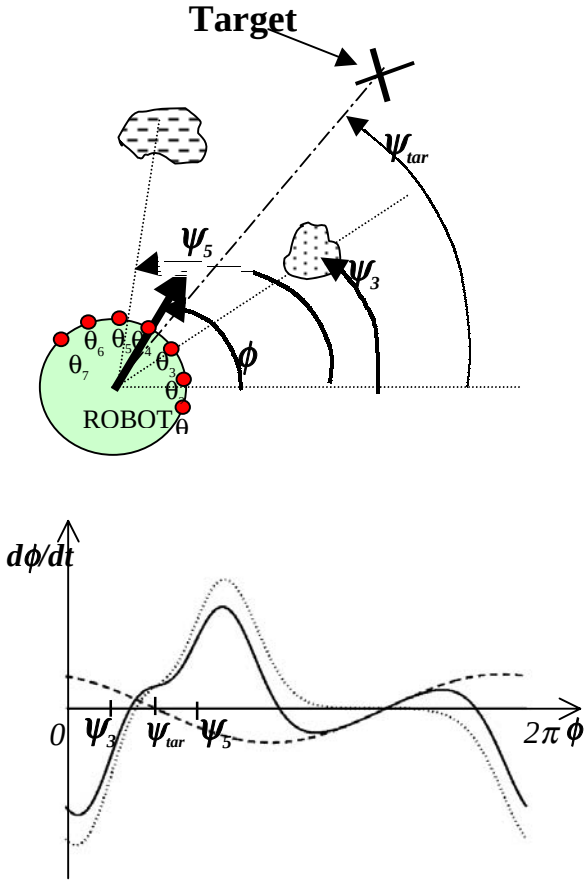

Figure 6. On the top: distance between obstacles is not sufficient for the robot to pass through them, and a target exists in the direction pointing in between the two obstacles thus defying the obstcale avoidance behavior. On the bottom: obstacle and target contributions for the dynamics by doted and traced curves respectively. The resulting dynamics is the continuous line.

C. *Path velocity control*

As the robot moves sensory information changes and thus attractors for heading direction shift. The same happens if obstacles or targets move in the world. Since the system must be at all the times in or near an attractor, i.e. a stable state, we must limit the rate of such shifts, so that the system can stabilize to the attractors as they move. This can be accomplished by controlling the driving speed, v, of the robot such as to stabilize a particular "time to contact", $T_{2c} = d/v$, where d is the distance to an obstruction or to the target.

If the parameter, $T_{2c} = d/v$, is chosen much larger than the typical relaxation time of the heading direction dynamics, then typically the system will have enough time to relax to the attractor before a strong change in the relationship of the robot to its environment is incurred. These constraints of keeping the time to contact constant, either with the obstacles or with the target, is achieved be the a dynamics for the path velocity

$$\frac{dv}{dt} = g_{obs}(v) + g_{target}(v) \qquad (8)$$

consisting of two contributions. Here each contribution is an attractive force erected at the required velocity, v_i, with strength c_i, and range σ_i, (i=obs or target)

$$g_i = -c_i (v - v_i) \exp\left[\frac{(v - v_i)^2}{2\sigma_v^2}\right] \qquad (9)$$

The times scales are adjusted through choice of ci such that in the presence of strong obstacle contributions the obstacle term dominates while in the absence of such contribution the target term dominates, for further details see (Bicho, Schöner, 1997a).

D. *Implementation*

In implementation, the dynamics of heading direction and path velocity are integrated numerically (Euler) simultaneously with the dead-reckoning equations. Both Ir and sonar sensors are used. For each Euler time step five sonar measures, for each sonar, are done and from these the average distance is computed. . Sonars range is from *0.45 m* to *1.75 m* while Infra-red's maximum range *0.6 m*. The *sensor fusion* between Infra red and sonars is performed through a very simple algorithm In the overlap distances interval the minimum distance is taken as the estimated distance to an obstacle. The heading direction dynamics depends on the current distance readings from the sensors, which are updated at each Euler step. The rate of change of heading direction specifies the angular velocity of the robot (i.e. $\omega_{robot}=d\phi/dt$). From this and the path velocity, v, the rotation speeds of the left and right wheels can be computed. The speeds are set as set point for the motor velocity servos. Parameters are set choosing the adequate times scale relation that makes the system to be at all times in a stable state. For details see Steinhage, Schöner, 1997.

IV RESULTS

Figure 7 and Figure 8 show sample trajectories of the robot as recorded by the dead-reckoned robot position. The target is placed behind the vehicle at coordinates (x_{target},y_{target}) = (1.0, 2.2) *m* with respect to its initial position. The vehicle stops running when the estimated distance from the center of the vehicle to the target is

equal to *30 cm*. The error in this estimated distance and the real distance varies between *10* and *20 cm* depending on the length of the overall path. For the trajectories shown in Figure 7 infra-red sensors and sonar sensors were used. In the first run (top of Figure 7), as one can see, the robot immediately turns toward the target position. In the second run (bottom of Figure 7) two obstacles, indicated by **A**, are placed to the right of the robot with respect to its departure position. These obstacles make the robot turn initially left to avoid them and not directly toward the target as before. Then the robot attempts to reach the target through the left direction. However it detects that this way is a dead-end (**B**). Therefore it changes the direction of driving and as one can see successfully reaches the target. In Figure 8 the environment from the previous run was kept exactly equal but this time only infra-red sensors are used. Here the robot approaches closer the obstacles referred as **B** because the Infra-red sensors range is *60 cm.* When sonars are also used the robots starts seeing the obstacles for larger distances and therefore it can anticipate which direction to move. In Figure 8 the dead-end is detected later.

As we can from the results the dynamic path planning system leads to smooth collision free trajectories to the target.

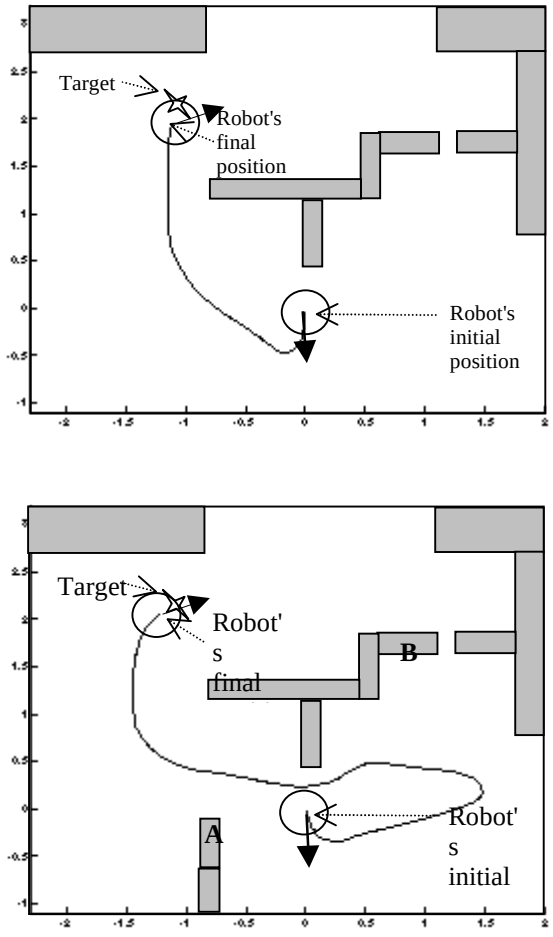

Figure 7. Two sample trajectories of the robot as recorded by the dead-reckoned robot position The target is placed at coordinates *(1.0,2.2) m* from its initial position. In the bottom the robot behavior is further constraint initially through obstacles **A**. Here sonars and Infra-red sensors are used.

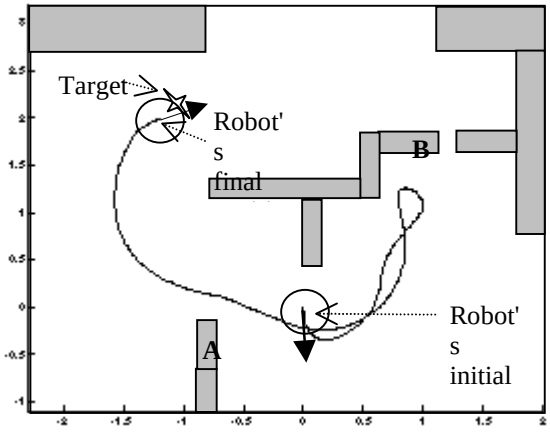

Figure 8. Another sample trajectory of the robot as recorded by the dead-reckoned robot position with the use of Infra-red sensors only.

V DISCUSSION

The dynamic approach to path generation of autonomous vehicles can be used even in the absence of veridical representation of obstacles as objects in the world. The information from distance sensors is directly used to define contributions to a dynamical system of heading direction and also to a dynamical system of path velocity. Heuristically, the sum over such contributions has attractors that specify collision free directions toward the target.

VI ACKNOWLEDGEMENT

This project was supported, in part, through grant BD/2949/94 from the PRAXIS program. We would like like to thank Prof. Francisco Vaz for making this collaboration possible, Prof. Carlos Couto for his institutional support. Discussions with Axel Steinhage, Wolfram Erlhagen and Martin Giese are gratefully acknowledged. Finally we would like to thank Bernard Arnaud (from CNRS / CRNC) Yvan Cecere and Loic Davy (from CNRS / CTM) for their help on the mechanical parts.

VI REFERENCES

Latombe, 1991; Latombe, J. C, "Robot Motion Planning", Kluwer Academic Publishers}, 1991.

Cox, Wilfong, 1990; Cox, I J and Wilfong, G T, "Autonomous robot vehicles", Springer Verlag, Berlin,1990.

Kedem, Sharir, 1988; Kedem, K and Sharir, M, "An automatic motion planning system for a convex polygonal mobile robot in 2-dimensional polygonal space", Proceedings of the 4th Annual Symposium on Computational Geometry Association for Computing Mashinery, 239-340, 1988, reprinted in Cox and Wilfong (eds.) (1990).

Khatib, 1986; Khatib, O, "Real-time obstacle avoidance for manipulators and mobile Robots", International Journal Robotics Research, 5, 90-98, 1986.

Schöner, Dose, 1992; G. Shöner, M.Dose, " A dynamical system approach to task level system integration used to plan and control autonomous vehicle motion", Robotics and Autonomous Systems, vol.10, pp. 253-267, 1992.

Schöner, Dose, Engels, 1995; G. Schöner, M.Dose, C. Engels " Dynamics of behavior theory and applications for autonomous robot architectures", Robotics and Autonomous Systems, vol.16, pp. 213-245, 1995.

Bicho, Schöner, 1997 ; E. Bicho, G. Schöner, " The dynamic approach to autonomous robotics demonstrated on a low-level vehicle platform", Robotics and Autonomous Systems, vol.21, pp. 23-35, 1997.

Bicho, Schöner, 1997a; E. Bicho, G. Schöner, " Target position estimation, target acquisition and obstacle avoidance", ISIE'97, vol.21, SS13-SS20, Guimarães, Portugal, July 7-12,1997.

Steinhage, Schöner, 1997; A. Steinhage, G. Schöner, " The dynamic approach to autonomous robot navigation", ISIE'97, vol.21, SS7-SS12, Guimarães, Portugal, July 7-12,1997.